Mol Cell Biochem
DOI 10.1007/s11010-017-3158-y

Cellular and molecular oxidative stress-related effects in uterine myometrial and trophoblast-decidual tissues after perigestational alcohol intake up to early mouse organogenesis

Tamara Anahí Coll[1,2] · Gabriela Chaufan[1,3] · Leticia Gabriela Pérez-Tito[1,2] · Martín Ricardo Ventureira[1,4] · María del Carmen Ríos de Molina[1,3] · Elisa Cebral[1,4,5]

Received: 9 March 2017 / Accepted: 5 August 2017

Abstract The placenta plays a major role in embryo-fetal defects and intrauterine growth retardation after maternal alcohol consumption. Our aims were to determine the oxidative status and cellular and molecular oxidative stress effects on uterine myometrium and trophoblast-decidual tissue following perigestational alcohol intake at early organogenesis. CF-1 female mice were administered with 10% alcohol in drinking water for 17 days prior to and up to day 10 of gestation. Control females received ethanol-free water. Treated mice had smaller implantation sites compared to controls ($p < 0.05$), diminished maternal vascular lumen, and irregular/discontinuous endothelium of decidual vessels. The trophoblast giant cell layer was disorganized and presented increased abnormal nuclear frequency. The myometrium of treated females had reduced nitrite content, increased superoxide dismutase activity, and reduced glutathione (GSH) content ($p < 0.05$). However, the trophoblast-decidual tissue of treated females had increased nitrite content ($p < 0.05$), increased GSH level ($p < 0.001$), increased thiobarbituric acid-reactive substance concentration ($p < 0.001$), higher 3-nitrotyrosine immunoreaction, and increased apoptotic index ($p < 0.05$) compared to controls. In summary, perigestational alcohol ingestion at organogenesis induced oxidative stress in the myometrium and trophoblast-decidual tissue, mainly affecting cells and macromolecules of trophoblast and decidual tissues around early organogenesis, in CF-1 mouse, and suggests that oxidative-induced abnormal early placental formation probably leads to risk of prematurity and fetal growth impairment at term.

Keywords Placenta · Decidua · Oxidative stress · Cellular and tissue damage · Mouse organogenesis · Perigestational alcohol

✉ Elisa Cebral
ecebral@hotmail.com

[1] Facultad de Ciencias Exactas y Naturales, Universidad de Buenos Aires, Buenos Aires, Argentina

[2] CONICET-Universidad de Buenos Aires, Buenos Aires, Argentina

[3] Departamento de Química Biológica, Instituto de Química Biológica de la Facultad de Ciencias Exactas y Naturales (IQUIBICEN), CONICET-Universidad de Buenos Aires, Buenos Aires, Argentina

[4] Instituto de Biodiversidad y Biología Experimental y Aplicada (IBBEA), CONICET-Universidad de Buenos Aires, Buenos Aires, Argentina

[5] IBBEA-UBA/CONICET, Intendente Güiraldes, 2620, Ciudad Universitaria, Pabellón 2, 4to. Piso, Lab 22. (CP: 1428EGA), Ciudad Autónoma de Buenos Aires, Buenos Aires, Argentina

Introduction

Maternal alcohol consumption can lead to the irreversible condition of fetal alcohol syndrome (FAS), described for the first time by Jones and Smith (1973) [1]. FAS, which represents only part of the spectrum of alcohol spectrum disorders (FASDs) [2, 3]; it is characterized by multiple fetal and birth disorders, such us intrauterine growth retardation (IUGR), craniofacial malformations, physical and mental retardation, behavioral and neurocognitive disabilities, delayed prenatal and postnatal growth, abnormal development of heart, limbs, and central nervous system. In addition to FAS, prenatal alcohol exposure (PAE) may cause a spectrum of disorders including neurodevelopment impairment without facial features. Rates of PAE appear to be increased in populations with other risks

Published online: 18 August 2017

associated with poor outcomes including poverty, poor diet, smoking, and limited access to prenatal care and advanced obstetric facilities [4]. Considerable differences between countries in prevalence estimations for FASD were found. Current prevalence estimates for FASD range from 0.5 (FAS only) to 1–30 cases per 1000 live births for all FASD in the USA. The mortality rates of FASD range from 4 to 5%, and the maternal mortality rate over a 10-year period is about 4.5% [9]. In Africa, some areas have a rate of FASD in live born infants of 4% or higher [4]. Particularly high prevalence rates were observed in South Africa for FAS (55.42 per 1000), for alcohol-related neurodevelopmental disorder (20.25 per 1000), and FASD (113.22 per 1000) [5]. Popova and colleagues [6] reported very high global prevalence rates of alcohol use in pregnancy (9.8%) and FAS (14.6 cases per 10,000). Of every 10,000 people in the general population globally, 15 will have FAS, and at least 10% of women continue to expose their unborn babies to alcohol. One in every 67 women who consume alcohol during pregnancy will have a child with FAS. Of annual pregnancies in the USA, about 40% of women drink some alcoholic beverage during pregnancy and about 3–5% of women drink heavily throughout pregnancy. Frequent alcohol drinking in the third trimester of pregnancy was estimated at 4.6%. However, many women continue to drink during the early stages of pregnancy while unaware they are pregnant. Approximately 12.2% pregnant women reported using alcohol during their pregnancy and nearly 2% reported binge drinking.

Our understanding of the pathophysiologic mechanisms of PAE is still incomplete. Some animal models of PAE suggested a relationship between abnormal placenta and risk for adverse embryo development, pregnancy outcomes [7], IUGR, and congenital defects associated with FAS [8]. High-dose ethanol can inhibit fetal growth, while low and moderate dose ethanol had the opposite effect, which could be explained, at least in part, by changes in placental efficiency. Both extremes of birth weight increase the risk in adulthood of obesity, metabolic syndromes, fetal programming diseases, and epigenetic effects [9]. Decreased placental size, impaired blood flow and nutrient transport, endocrine changes, increased rates of stillbirth and abruption, fetal resorption, umbilical cord vasoconstriction, and low birth weight were seen after severe chronic ethanol consumption during pregnancy [4, 9]. Extraembryonic tissues and yolk sac were also affected after acute alcohol exposure [10]. Repeated binge exposures adversely affect maternal uterine vasculature whereas moderate exposures impair uterine artery vasodilation [9]. Despite this evidence, further studies are needed to determine both whether maternal alcohol ingestion previous to gestation disrupts early placentation and also the mechanisms involved.

The placenta is a vital and crucial organ of pregnancy for nutrient delivery, gas and hormone exchanges, and waste removal at the maternal–fetal interface. Placentation begins with implantation during the early stages of gestation. During gastrulation (7–8.5 days of mouse gestation), trophoblast cells of the ectoplacental cone differentiate into trophoblast giant cells (TGCs) while mononuclear trophoblast cells proliferate. As long as TGCs make contact with the uterine wall and invade the endometrium to degrade the underlying extracellular matrix, the adjacent endometrial stroma undergoes decidualization. At this time, a specialized and vascularized tissue encapsulates the developing embryo to provide nutrients and controls the trophoblast invasion. By mid-placentation in mouse, at early organogenesis (day 10–11 of gestation), the hemotrichorial placenta consists of three zones of trophoblast layers that are differentiated at the mesometrial side of the implantation site: the chorionic and mononuclear trophoblast of labyrinth, the spongiotrophoblast layer, and the trophoblast giant cell zone [11]. On the mesometrial side of the implantation site, the lumen of the spiral arteries of the decidua increases to allow high flow and continuous nutrient supply through the trophoblastic area to the embryo [11]. This event is accompanied by a sharp rise in O_2 tension and an increase in reactive oxygen species (ROS) in maternal tissue, which marks the establishment of full maternal arterial circulation to the placenta. At physiological concentrations, ROS stimulate cell proliferation and up-regulate antioxidant gene expression and activity to protect the fetal tissue against the deleterious effects of ROS during the critical phases of embryogenesis and organogenesis [12]. However, similarly to what occurs in complicated pregnancies with intrauterine growth restriction, pre-eclampsia, gestacional, diabetes, spontaneous abortion, recurrent pregnancy loss, and other placentopathies related to oxidative stress (OS) [12–15], this oxidative mechanism also seems to operate in placental pathology associated with maternal alcohol ingestion [16, 17].

Oxidative stress is caused by an imbalance between levels of ROS and/or reactive nitrogen species (RNS) and alterations in antioxidant defenses [18]. Reactive oxygen species are generated during crucial processes of oxygen consumption. Primary elimination of ethanol occurs through an oxidative mechanism via hepatic metabolism [19]. Upon ingestion, alcohol undergoes dehydrogenation to acetaldehyde [20]. Subsequent further dehydrogenation of acetaldehyde produces acetic acid with acetyl and methyl radicals. These metabolites are responsible for ROS generation, species overproduced with regular alcohol use [20]. ROS include nitric oxide (NO), nitrogen dioxide (NO_2), peroxynitrites (ONOO-), and nitrosamines [12].

Oxidative stress via NO production is involved in many physiological regulatory functions of the placenta (hemodynamic processes, vasodilatation, cell survival, and angiogenesis) [21]. However, excessive NO leads to pathological processes [12]. High NO levels can affect protein structure, function, and enzyme activity, alter cytoskeletal organization, and impair cell signal transduction [22, 23], since actions of NO are dependent on its levels, the redox status of the cell, and quantities of metals, proteins, and thiols, among other factors [24]. The reaction between NO and SO anions leads to generation of the powerful, reactive peroxynitrite anion. This species is able to inhibit mitochondrial electron transport, inducing lipid peroxidation and nitrosation of the tyrosine amino acid of many tyrosine molecules that normally act as mediators of enzyme function and signal transduction [24, 25].

In order to prevent ROS-induced cellular damage, a variety of antioxidant mechanisms can be activated to maintain the oxidant/antioxidant balance. Antioxidants may be enzymatic or non-enzymatic. Endogenous non-enzymatic antioxidants include different thiol compounds, such as glutathione (GSH), and enzymatic antioxidants include, among others: superoxide dismutase (SOD) enzymes, catalase (CAT) [26], and the glutathione family of enzymes (GP*x*, GST, and GSH reductase). Glutathione peroxidase (GP*x*) uses the reduced form of glutathione as an H^+ donor to degrade peroxides. Depletion of GSH results in DNA damage and increased H_2O_2 concentrations [27]. During reduction of H_2O_2, GSH is oxidized to nombre complete (GSSG) by GPx. Ethanol exposure alters levels of intracellular antioxidants, such as glutathione (GSH), CAT, SOD, and GSH S-transferase (GST) [28].

Understanding of the effects and pathophysiologic mechanisms of early placentation after moderate alcohol ingestion up to organogenesis is still incomplete. This is important since most women often drink alcohol before learning that they are pregnant (4–6 weeks' gestation) [29] and/or even with 10–12 weeks of gestation during organogenesis. Therefore, we recently established a mouse model for studying embryonic effects of perigestational alcohol ingestion up to early organogenesis. At this gestational time, embryonic stage E10, the most advanced not-delayed stage of early organogenesis in mouse, is the embryonic stage that will continue development to term. Since congenital defects related to prenatal alcohol exposure are most likely to originate in this organogenic period, we have recently been interested in the study of effects and mechanisms of alterations of E10 embryos exposed to alcohol [30–32]. In our outbred mouse, perigestational alcohol ingestion up to day 10 of gestation leads to more delayed embryos and reduced frequency of organogenic E10 embryos with increased dysmorphology [31], defective regulation of prostaglandin-NO pathways, altered expression of cell protein adhesion [30, 31], and increased oxidative stress [32]. However, we do not know about cellular and molecular effects of moderate perigestational alcohol intake on maternal-placental tissues during placentation in early organogenesis in outbred mice. We chose the outbred mouse model because it represents the variability of alcohol response in humans given its high genetic polymorphism. We focused on this embryonic stage because a moderate quantity of ethanol ingestion is the most common alcohol concentration used by alcoholic women which can produce placentopathy [4].

Our hypothesis was that moderate perigestational alcohol intake produces, in the outbred mouse, histomorphological alterations in decidual and trophoblast tissues of the implantation site at organogenesis, and ethanol-induced oxidative stress and increased cellular and macromolecular damage which may explain decidual and trophoblastic tissue alterations. The aim of our present work was to determine oxidative status in uterine myometrium and trophoblast-decidual (T-D) tissues after perigestational alcohol treatment up to day 10 of gestation in CF-1 mouse, analyzing nitric oxide species, antioxidant defense levels, and OS-impact on histo-morphology, proteins, lipids, and DNA of maternal-placental tissues after perigestational alcohol exposure.

Materials and methods

Animals

Conventional sexually mature stock of outbred CF-1 mice (CrlFcen:CF1, Mouse Genome Informatics (MGI)), produced by FCEN [School of Exact and Natural Sciences] of the University of Buenos Aires (Buenos Aires, Argentina) were used. Three to five female mice were housed in groups in separate same-sex communal cages and kept on a 22 °C and light/dark cycle (14 h:10 h). They were fed commercial mouse chow (*Alimento*"*Balanceado Cooperación Rata-Ratón*" from the *Asociación Cooperativa de Alimentos S.A. Buenos Aires, Argentina*) and tap water, hyperchlorinated to 3–5 ppm, ad libitum. CF-1 female mice were 60 days old and average body weight was 27–30 g at the outset of ethanol treatment.

Alcohol experimental design

Experiments were carried out according to the regulation and ethical standards of the Institutional Animal Care and Use Committee (IACUC, protocol Nr 57), of the Facultad de Ciencias Exactas y Naturales, Universidad de Buenos Aires (FCEN-UBA, Argentina) and in accordance with the guidelines of the National Institute of Health.

Adult female mice were orally exposed to 10% (w/v) ethanol in drinking water for 17 days previous to mating and up to day 10 of gestation. Control CF-1 females received ethanol-free drinking water ad libitum. This perigestational ethanol paradigm produced a blood alcohol concentration (BAC) of 24 mg/dL at day 10 of gestation and significantly increased embryo resorption, delayed embryo development, and high frequency of organogenically abnormal embryos [31]. In this mouse model, to synchronize mating of control and treated groups, females were superovulated on day 15 of treatment with intraperitoneal injection of 5 IU equine Chorionic Gonadotropin (eCG; *Novormon, Syntex S.A., Argentina*) at 13:00 h followed by an i.p. injection of 5 IU of human Chorionic Gonadotropin (hCG; *Sigma Chemical Company*) 48 h later (day 17 of treatment). At hCG injection, females were caged individually with a male overnight and on the following morning were checked for presence of vaginal plug, when day 1 of pregnancy was assumed. Then, CF-1-mated females were housed again with administration of 10% ethanol, and gestation continued up to day 10. CF-1-control females received ethanol-free drinking water during the same period of ethanol treatment, were mated, and allowed to continue gestation up to day 10 of gestation.

Control and ethanol-treated pregnant female mice were weighed at the beginning and at the end of ethanol treatment. Every day in the morning, volume of liquid drunk and quantity of food consumed were recorded to monitor amounts of daily liquid, food, and calorie intake (estimated by calorie value of the diet used (3976 kcal/kg) and calories derived from ethanol (estimated as 7.1 kcal/g). From these data, mean calorie intake and percentage of ethanol-derived calories (% EDC) were estimated for each experimental group. At least 5 pregnant mice per experimental group for each study were used.

Tissue collection and processing

On the morning of day 10 of gestation, control and treated females were killed by cervical dislocation and the abdominal cavity was surgically opened to quickly remove the uteri which were placed in Petri dishes with Krebs–Ringer Bicarbonate solution (KRB) (11.0 mM glucose, 145 mM Na^{+}, 2.2 mM Ca^{++}, 1.2 mM Mg^{++}, 127 mM Cl^{-}, 25 mM HCO^{3-}, 1.2 mM SO_4^{2-}, and 1.2 mM PO_4^{3-}). Implantation sites were isolated under a stereomicroscope (Wild Heerbrugg Photo mikroskop M400, 2X) for immediate fixation in paraformaldehyde 4%/PBS for 18 h at 4 °C, and the uterine and decidual tissues and the developing embryo within it were dissected. The stage of embryonic development was determined by observation under stereomicroscopy [31] considering the external appearance of neural tube, body flexure, forelimb buds, number of branchial arches, and number of somites. At day 10 of gestation, the main normal embryo stage of development is the E10 embryo (14–20 somites, with a beating heart and closed neural tube). Only uterine myometrial and trophoblast-decidual tissues from implantation sites containing embryos at E10 stage were collected and immediately stored at −70 °C for oxidative stress studies. Reabsorbed implantation sites (staged at E7 to E8.5 with necrotic and/or hemorrhagic trophoblast-decidual tissue) or implantation sites with retarded embryos (E9) were not included in the study.

Histology

Fixed implantation sites were dehydrated by increasing concentrations of alcohol solutions followed by immersion in xylene, and embedded in *Paraplast.* Transverse central sections of implantation sites containing an E10 embryo in the cavity were performed by cutting (7 μm thick) perpendicularly to the longitudinal axis of the uterus. Only the central sections were used, with the aim of including the largest area of decidua. Slices were adhered onto glass slides by 0.1% poly-L-Lysine (Sigma, MO, USA), and sections were deparaffinized in xylene, hydrated by decreasing concentrations of ethanol, and stained with hematoxylin and eosin according to standard protocols.

Morphometry and histopathology of the implantation site

The stage of the embryo in the cavity was evaluated in each section of implantation site by the embryo's histological characteristics. We observed development of heart, somites, the cephalic neural tube, and the general aspect of embryo in relation to its axial rotation and position of the allantois. Only implantation sites containing an E10-staged embryo (E10-IS) were selected for morphometrical and histological analysis. Both retarded implantation sites (containing an E9 embryo with low development of neuroepithelium of neural tube, non-axially rotated embryo, and reduced growth of allantois) and reabsorbed implantation sites (with necrotic tissue, hemorrhage, blood congestion, and severely retarded embryo development) were rejected for morphometrical analysis.

Morphometry of implantation sites was performed on digital images of transverse and central sections of E10-IS obtained with an Axiophot Zeiss microscope (Carl Zeiss, Inc. Oberkochen, Germany) equipped with a camera driven by Olympus DP71 with an image analyzer Olympus cellSens software (Olympus, Tokyo, Japan). The areas (Fig. 1a) and lengths (Fig. 1b) of tissue regions were measured by Image *Pro Plus* software (Media Cybernetics Inc., Silver Spring, MD). Using calibration references for

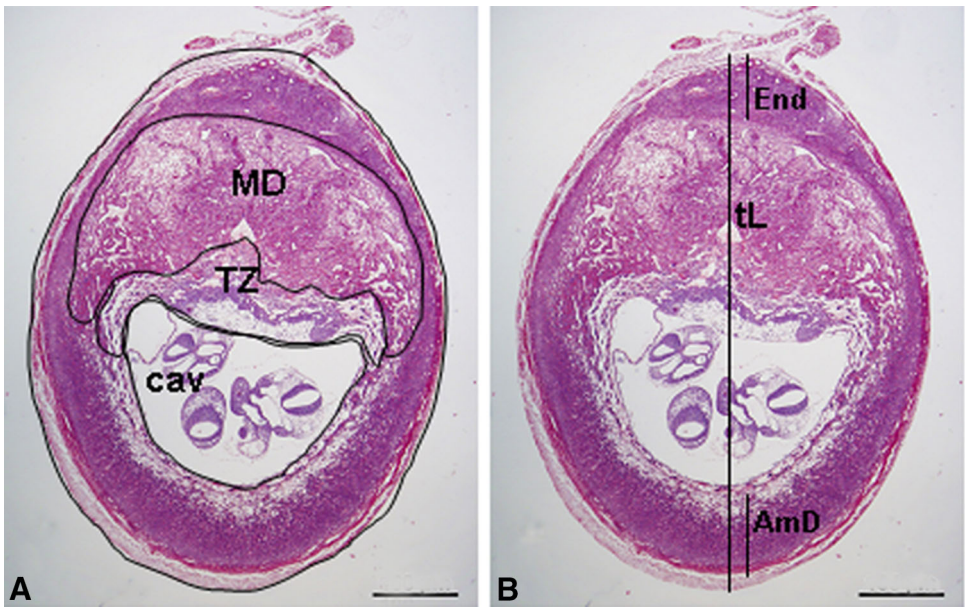

Fig. 1 Morphometric analysis of the E10-implantation site. Morphometry of histological sections of E10-IS (*Image Pro Plus*). **a** Areas of mesometrial decidua (MD), trophoblastic zone (TZ), and embryo cavity (cav). **b** Lengths of non-decidualized endometrium (End), antimesometrial decidua (AmD), and total length of the implantation site (*scale bar* 700 μm)

total magnification of the optical system, the total length (μm) of the implantation site was determined by taking a line from the outer edge of the antimesometrial myometrial side to the outer edge of the mesometrial myometrial side. Total area of the implantation site (measured from the outer edges of the myometrium, μm^2), the areas of the different components (the cavity, the mesometrial decidua, the trophoblast area), and the lengths (antimesometrial decidua, mesometrial non-decidualized endometrium), were normalized to the total value of area or length, respectively. Results were expressed as mean size (μm or μm^2) and standard deviation of central implantation site sections derived from $n = 9$ females for control group and $n = 10$ females for ethanol-treated group.

The histopathology of mesometrial decidua and trophoblastic zone of the E10-implantation site was analyzed. In the proximal decidua, the general histo-morphology, degree of expansion of maternal blood vessel lumen, and endothelial cells lining the lumen of decidual vessels were evaluated. In trophoblastic zone, the histological aspect of labyrinth, the spongiotrophoblastic and trophoblast giant cell layer were analyzed. Two implantation sites per litter from at least 4 control and 4 ethanol-exposed dams were included in the histopathological study.

Hoechst 33,342 staining

The DNA stain Hoechst 33,342, which binds preferentially to A-T base-pairs, was used for labeling nuclei of trophoblast giant cells and endothelial cells of decidual vessels in E10-IS. Briefly, deparaffinized sections were rinsed three times in PBS and incubated with 0.5 μg/ml Hoechst 33,342 (Sigma Chemical Co., USA) in PBS for 1 min in darkness. After further rinses in PBS, sections were coverslipped with a solution of glycerol in PBS (1:1). Normal and abnormal nuclei of trophoblast giant cells were evaluated in images (40x) obtained with an Axiophot Zeiss microscope. In the two fields of trophoblast giant cell layer per E10-IS from a female, the number of regular ovoid nuclei, the chromatin-condensed nuclei and fragmented, over the total number of nuclei, were quantified and expressed as frequency (%). In proximal decidua, morphology of endothelial nuclei and alignment to basal membrane of maternal blood vessels were analyzed.

Antioxidant enzyme activities

Explants of uterine myometrium and trophoblast-decidual tissue were defrosted and whole homogenates of each tissue sample were prepared in 0.154 M KCl (1:5, w/v) containing protease inhibitors (0.5 mM PMSF and 0.2 mM benzamidine). Then, samples were centrifuged for 20 min at $10{,}000 \times g$ and aliquots of supernatant were separated for each determination.

Catalase activity (CAT)

Catalase (EC 1.11.1.6) activity was determined by following hydrogen peroxide (H_2O_2) dismutation at 240 nm, in a reaction mixture containing 50 mM potassium phosphate buffer (pH 7.0) and 30 mM H_2O_2 [33]. One CAT unit was defined as the enzyme amount that transforms 1 mmol of H_2O_2 per min. Results were expressed as mean enzymatic units per g tissue.

Glutathione S-transferase (GST)

Glutathione S-transferase (EC 1.11.1.9) activity was measured as previously [34]. Briefly, standard assay mixture is formed by adding to the enzymatic sample 100 mM GSH solution, and 100 mM 1 chloro-2, 4-dinitrobenzene (CDNB) in ethanol, in 100 mM phosphate buffer (pH 6.5), to a final volume of 0.8 ml. After adding CDNB, change in absorbance at 340 nm was followed for 180 s every 30 s. Results were expressed as units per mg of proteins. One GST unit was defined as the amount of enzyme that catalyzes the formation of 1 µmol of GS-DNB per minute.

Superoxide Dismutase (SOD)

Superoxide Dismut*ase* (EC 1.15.1.1) activity was measured by a modified Beauchamp and Fridovich [35] procedure in microplate. The standard assay mixture contained enzymatic sample, 0.1 mM EDTA, 13 mM DL-methionine, 75 µM nitro blue tetrazolium (NBT), and 2 µM riboflavin, in 50 mM phosphate buffer (pH 7.9), to a final volume of 0.3 ml. Samples were exposed 5 min to intense cool white light. Results were expressed as units per mg of proteins. One SOD unit was defined as the enzyme amount necessary to inhibit the reaction rate by 50%. Samples were measured at 560 nm in a Bio-Rad Benchmark microplate reader (Bio-Rad Laboratories, Hercules, CA). Results were expressed as mean enzymatic units per g tissue.

Reduced glutathione (GSH) content

GSH content was measured by the Anderson procedure (1985) [36] with some modifications. Briefly, samples were acidified with 10% sulfosalicylic acid. After centrifugation at 8000×*g* for 10 min, supernatant (acid-soluble GSH) aliquots were mixed with 6 mM 5,5-dithiobis-(2-nitrobenzoic) acid (DTNB) in 0.143 M buffer sodium sulfate (pH 7.5) containing 6.3 mM EDTA. Absorbance at 412 nm was measured after 30 min incubation at RT. GSH content was determined by standard curve generated by a known GSH amount. Results were expressed as nmol GSH per mg of tissue.

TBARS determination

Lipid peroxidation was assessed by measuring concentrations of thiobarbituric acid-reactive substances (TBARS) using a modified Buege and Aust procedure [37]. Briefly, approximately 150 mg of tissue were homogenized in 0.154 M KCl (1:5 w/v) containing 0.5 mM PMSF and 0.2 mM benzamidine, as protease inhibitors. The homogenates were centrifuged at 11,000×*g* for 20 min at 4 °C, and resulting supernatants were used for TBARS determinations. An aliquot of 0.2 ml was mixed with thiobarbituric acid (1 ml, 0.375% w/v) solution (Sigma-Aldrich Co.), and the solution heated at 100 °C for 40 min. Then, samples were cooled for 5 min in ice, centrifuged for 5 min at 10,000×*g*, and absorbance of supernatant was quantified spectrophotometrically at 535 nm. TBARS concentration was estimated using the extinction coefficient of MDA–thiobarbituric acid complex (156 mM^{-1} cm^{-1}). Results were expressed as nmol of TBARS per mg of tissue.

Nitrite content

NO production of myometrial and trophoblast-decidual tissues was evaluated by assaying the concentration of its stable metabolites nitrates/nitrites using a commercial kit (Cayman Chemical Company). Tissue samples were defrosted and homogenized in 500 µl Tris–HCl buffer 0.1 M, pH 7.4. Samples were centrifuged for 12 min at 3000×*g* at 4 °C and aliquots of supernatant were stored at −20 °C. In the supernatant, nitrates were reduced to nitrites by nitrate reductase, and total nitrites were measured by the Griess method [38]. Optical densities were measured at 570 nm in a microliter plate using $NaNO_3$ and $NaNO_2$ as standards. Results were expressed as mean µmol NO_2/mg protein and standard deviation.

Immunohistochemistry

Immunohistochemical analysis was run to detect 3-nitrotyrosine residues (3-NT). Implantation site slices were deparaffinized with xylene, rehydrated through a graded ethanol series, and washed in PBS. To expose the epitopes, slices were heated in 10 mM sodium citrate in PBS (pH 6.0) in microwave (5 min at 400 W) and cooled in PBS. Sections were permeabilized with PBS–Triton X-100 (0.25%) for 15 min. After washing, endogenous peroxidase activity was blocked in 3% H_2O_2/PBS for 30 min at RT. Then, sections were washed and incubated in 3% non-fat dry milk/PBS at RT in a humid chamber for 1 h to inhibit unspecific staining. Primary antibody against 3-nitrotyrosine rabbit (Molecular Probes Inc., Leiden, Netherlands) was applied (1:50) in PBS and slices were incubated overnight at 4 °C. After washing, sections were incubated with biotinylated goat polyclonal antibodies against rabbit IgG (1:100) (Vector Laboratories, Burlingame, CA) in PBS for 1 h at RT. The reaction was enhanced with streptavidin, horseradish peroxidase-conjugated (Chemicon International Inc., Temecula, CA, USA) (1:100) for 1 h incubation at RT. Finally, samples were washed and treated for 2 min with 3–30-diaminobenzidine in chromogen solution (Cell Marque, Sigma). Slides were counterstained with hematoxylin and mounted in DPX Mountant for histology

(Sigma Chem. Co.). The slices were observed and photographed with an Axiophot (Carl Zeiss) light microscope. Specificity of staining was determined by incubating sections with PBS in the absence of the first antibody. Three entire sections per implantation site were examined by two skilled blinded observers.

TUNEL assay

For apoptosis analysis the Apoptag peroxidase in situ kit (Millipore S7101) was used. Sections of E10-IS, fixed in 4% paraformaldehyde, were deparaffinized and rehydrated in phosphate buffered saline (PBS). Then, they were permeabilized with PBS–Triton X-100 (0.5%) for 10 min and with Proteinase-K (20 µg/µl in PBS) for 15 min. Sections were post-fixed for 5 min with paraformaldehyde 4%, and endogenous peroxidase activity was blocked in 3% hydrogen peroxide/PBS for 5 min. After incubation in equilibration buffer, the tissue was placed in terminal deoxinucleotidil transferasa solution for 1 h at 37 °C in a humidified chamber. Sections were rinsed in stop buffer and then incubated in streptavidin-horseradish peroxidase solution for 10 min. Diaminobenzidine treatment for 2 min generated a brown-colored substrate. Sections were then counterstained with hematoxylin and mounted in DPX. Positive controls were obtained by incubating sections with DNAse 0.5% for 10 min at 37 °C. To quantify the number of TUNEL-positive cells, three entire sections of each tissue per E10-implantation site were examined by two skilled blinded observers, and the mean number of apoptotic cells was calculated for comparable sections of implantation sites for each group (number of females used = 5 for control and ethanol-treated group).

Statistical analysis

Reported values of mean ± SD of control and ethanol-treated samples were analyzed by Student's *t*-test. Values of frequency (Nr and %) were compared by Fisher´s exact test. For statistical analysis we used the GraphPad Instat v2.05a (GraphPAD Software Inc., San Diego, CA. USA). Differences between groups were considered statistically significant when $p < 0.05$.

Results

Ethanol consumption could produce body weight changes altering the pattern of food, liquid, and calorie intake. We monitored these parameters in the present mouse model during the period of treatment up to day 10 of gestation. The ethanol-treated females drank and ate a significantly reduced quantity of liquid and food compared to controls ($p < 0.001$, Table 1). The dose of ethanol consumed per day was 23.3 ml ethanol/kg or 0.64 ml per mouse, which represents 18.3 g ethanol/Kg (Table 1). During the ethanol exposure period, treated mice consumed the same amounts of total calories as controls, and 20% ethanol-derived calories of the total daily calorie intake was registered in treated females. No differences in body weight between the two groups were found (Table 1).

Histo-morphology of maternal-placental tissues after perigestational alcohol consumption

First, we observed the general development of implantation sites from control and ethanol-treated females. Figure 1a shows the areas of the implantation site, mesometrial decidua (MD), trophoblastic zone (TZ), and embryo cavity (cav); Fig. 1b depicts the lengths of the IS, non-decidualized endometrium, and antimesometrial decidua. Figure 2b shows that implantation site from treated female mice had altered tissue areas, indicated by reduced size of the trophoblastic zone and embryonic cavity area, and a larger size of the non-decidualized endometrium, compared to the same zones of implantation sites from controls (Fig. 2a). The morphometric analysis of areas and lengths of E10-IS revealed that E10-IS from ethanol-exposed females presented no changes in the size of the embryo cavity, nor in the areas of mesometrial and antimesometrial decidua, trophoblastic zone, and non-decidualized endometrium. Only the total area of the implantation sites, not including the uterine myometrial tissue, was significantly reduced in treated females compared to controls ($p < 0.05$) (Table 2).

The histo-morphology of mesometrial tissues of E10-IS was evaluated. The proximal decidua from ethanol-exposed females showed histological alterations with diminished vascular lumen of maternal blood vessels compared to the tissue of controls (Fig. 2e, c). Nuclear morphology in decidual tissue from treated females was irregular (Fig. 2f) compared to controls (Fig. 2d). In particular, the endothelium of decidual vessels from ethanol-exposed derived implantation sites was disorganized compared to the same tissue from controls (Fig. 2e, c). Concordantly, the alignment of endothelial nuclei to the lumen of blood vessels was irregular and discontinuous, resulting in the release of endothelial cells into the lumen (Fig. 2f, d).

E10-IS from ethanol-treated females presented a disorganized trophoblast giant cell layer compared to that of controls (Fig. 3c, a, respectively). Also, a significantly higher frequency of non-ovoidal nuclei was observed in treated females compared to the frequency of these nuclei found in controls ($p < 0.05$, Table 3; Fig. 3d, b, respectively). However, percentages of trophoblast nuclear

Table 1 Food, liquid, and ethanol intake after perigestational alcohol consumption in CF-1 mouse

	Control females ($n = 15$)	Ethanol-treated females ($n = 15$)
Liquid ingestion		
ml/Kg/day	264.1 ± 15.6	187.1 ± 10.6***
ml/mouse/day	7.5 ± 0.5	5.2 ± 0.4***
ml OH/kg/day	0	23.3
ml OH/mouse/day	0	0.64
g OH/Kg/day	0	18.3
g OH/mouse/day	0	0.51
Kcal liq/kg/day	0	130.0 ± 7.5
Food ingestion		
g/Kg/day	212.1 ± 21.1	165.5 ± 17.1***
g/mouse/day	6.3 ± 0.6	4.9 ± 0.6***
Kcal/kg/day	644.6 ± 53.9	504.3 ± 51.4***
Total caloric value		
Total Kcal/Kg/day	644.6 ± 53.9	634.3 3 ± 58.9
% EDC	0	20.5%
Body weight		
Initial (D1) (g)	28.5 3 ± 1.2	27.1 ± 0.8
Final (D27) (g)	29.4 ± 0.6	29.1 ± 0.8

Quantities of liquid and food consumption in control and ethanol-treated females were measured during the period of ethanol treatment. Results were expressed as mean ± standard deviation of quantities of food (g and kcal), liquid (ml, g ethanol), and total calories per mouse, kg, and day

% EDC percentage of ethanol-derived calories. *N* = number of females used for ingestion value measurement

*** $p < 0.001$, Student's *t*-test

fragmentation and chromatin condensed were not different from those of controls (Table 2).

In view of these results, the next step was to determine if the altered histology of E10-IS after perigestational alcohol ingestion was detected together with oxidative stress in tissues of the implantation sites.

Perigestational alcohol intake up to day 10 of gestation modified oxidative stress parameters in maternal-placental tissues

Total nitrite content, a measure of the level of NO, of uterine tissue from treated mice, was significantly reduced while nitrite content of trophoblast-decidual tissue was increased, compared to respective control tissues ($p < 0.05$) (Fig. 4).

Antioxidant enzymatic activity and non-enzymatic scavenger content were measured in uterine myometrium and trophoblast-decidual tissues of control and ethanol-treated female mice. Although GST and CAT enzymatic activities showed no differences between the myometrial and trophoblast-decidual tissues of control and ethanol-treated females (Fig. 5a, b, respectively), SOD activity of uterine tissue from treated mice was significantly higher than that of controls ($p < 0.05$, Fig. 5a). Also, uterine myometrial tissue from treated females had a significantly reduced GSH content than that of controls ($p < 0.05$) (Fig. 6). However, the trophoblast-decidual tissues of treated group had a significantly higher level of GSH compared to control group ($p < 0.001$, Fig. 6).

Perigestational alcohol ingestion up to day 10 of gestation induced tissue-specific macromolecular and cellular changes

TBARS content, measured as evidence of lipid peroxidation, was significantly increased in the trophoblast-decidual tissue of treated versus control group ($p < 0.001$), while TBARS content in uterine myometrium was not different from controls (Table 4).

Analysis of tissue nitrosylation showed almost negative immunoreactivity for 3-nitrotyrosine residues in longitudinal and circular layers of myometrium from control and treated females (Fig. 7a, b, respectively). Instead, mesometrial decidua (Fig. 7d) and trophoblastic tissues (Fig. 7f) from treated females had higher immunostaining for 3-NT than controls (Fig. 7c, e).

Myometrial tissue of treated females presented no apoptotic cells (data not shown). Instead, the decidua of implantation sites from treated females presented

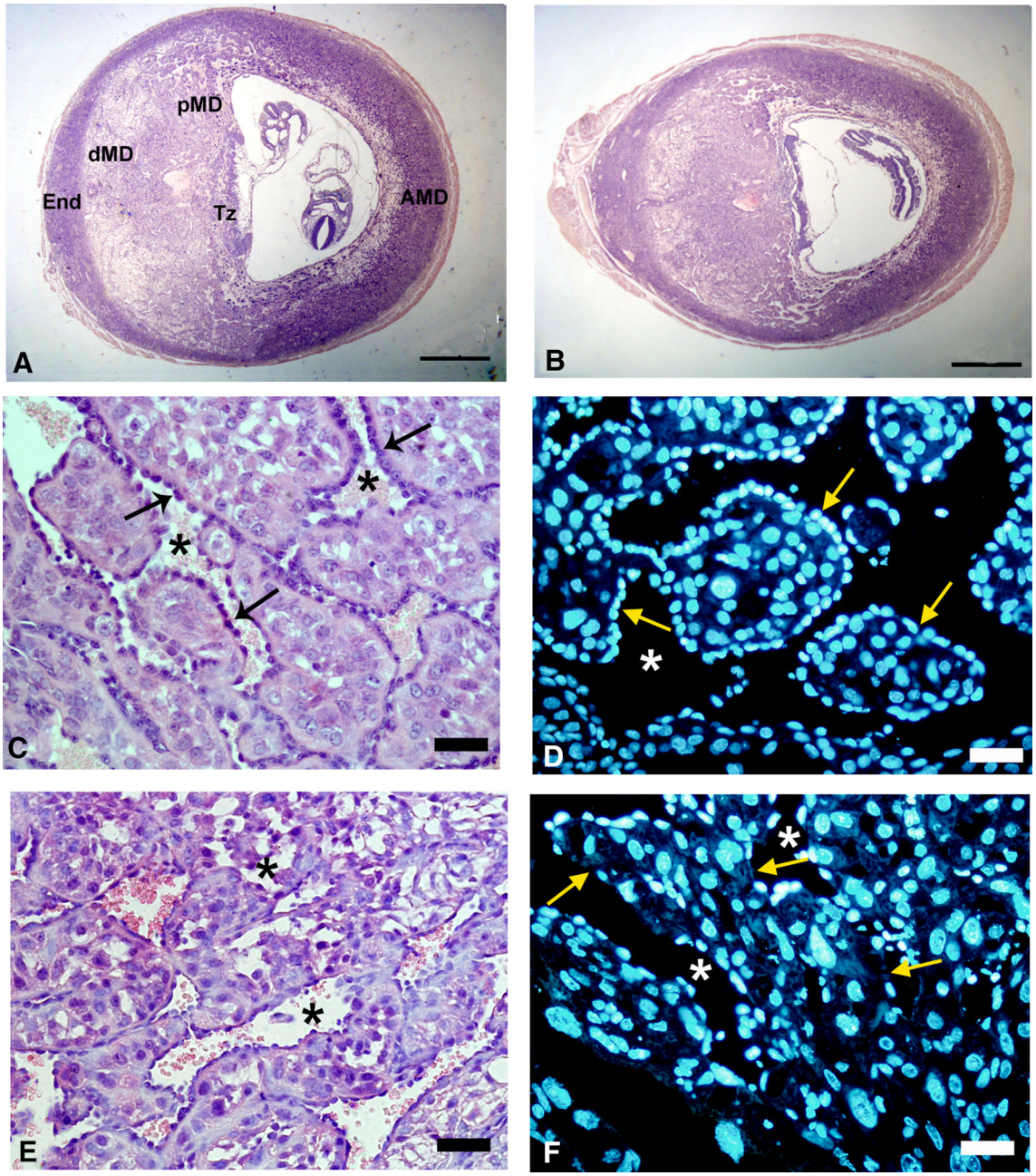

Fig. 2 Histological effects on decidual tissues after perigestational alcohol intake. Histology (H-E) and nuclear morphology (*Hoechst 33,342*) of decidua from E10-IS of control (CF) and ethanol-treated females (TF). **a** Representative implantation site from CF. **b** Representative implantation site from TF. **c** Representative histological image of mesometrial proximal decidua from CF, showing the lumen (*asterisk*) of maternal blood vessel lining by endothelial cells (*arrows*). **d** Representative images of ovoid endothelial nuclei limiting the lumen (*asterisk*) of maternal blood vessel of CF. **e** Representative histological image of proximal decidua from TF, showing histological alterations of decidual parenchyma and endothelial tissue (*arrow*). **f** Representative images of morphologically altered nuclei of decidua from TF, showing unaligned and/or absence of endothelial nuclei of maternal blood vessels (*asterisk*). *ndE* non-decidualized endometrium, *dMD* distal mesometrial decidua, *pMD* proximal mesometrial decidua, *AmD* antimesometrial decidua, *TZ* trophoblast zone (*scale bar*: **a**–**b**: 700 µm; **c**–**f**: 20 µm)

significantly increased numbers of TUNEL-positive cells compared to controls (Fig. 8b vs. a; Table 5). The trophoblast giant cell layer did not present increased apoptosis compared to the same layer in controls. However, the mononuclear trophoblast cells of labyrinths from treated females presented a significant higher number of apoptotic cells compared to controls (Fig. 8d vs. c). Table 5 shows that the total number of apoptotic cells in the trophoblastic

Table 2 Morphometry of implantation sites from control and ethanol-treated females at day 10 of gestation

	Control females	Ethanol-treated females
Female Nr	9	10
IS Nr	11	16
Mean IS-length Nr (mm)	4.59 ± 0.23	4.47 ± 0.35
Mean IS-area Nr × 10^3 (mm^2)	12.60 ± 1.14	11.01 ± 1.15*
Mean Cav-area/IS-area (mm^2)	2.73 ± 0.38	2.46 ± 0.77
Mean MD-area/IS-area (mm^2)	4.05 ± 0.71	3.53 ± 0.77
Mean TZ-area/IS-area (mm^2)	1.15 ± 0.27	1.13 ± 0.32
Mean End-length/IS-Length (mm)	0.09 ± 0.02	0.10 ± 0.02
Mean AmD-length/IS-Length (mm)	0.16 ± 0.02	0.16 ± 0.02

Transverse histological sections of E10-staged implantation sites from control and ethanol-treated females, were morphometrically processed. The mean number (Nr) of area (mm^2) or length (mm) of implantation site (IS), the embryo cavity (Cav-area), mesometrial decidua (MD), trophoblastic zone (TZ), non-decidualized endometrium (End), and antimesometrial decidua (AmD), over the total value or area or length of IS, was calculated in 9 control and 10 ethanol-treated females

* $p < 0.05$, versus control group, Student's *t*-test

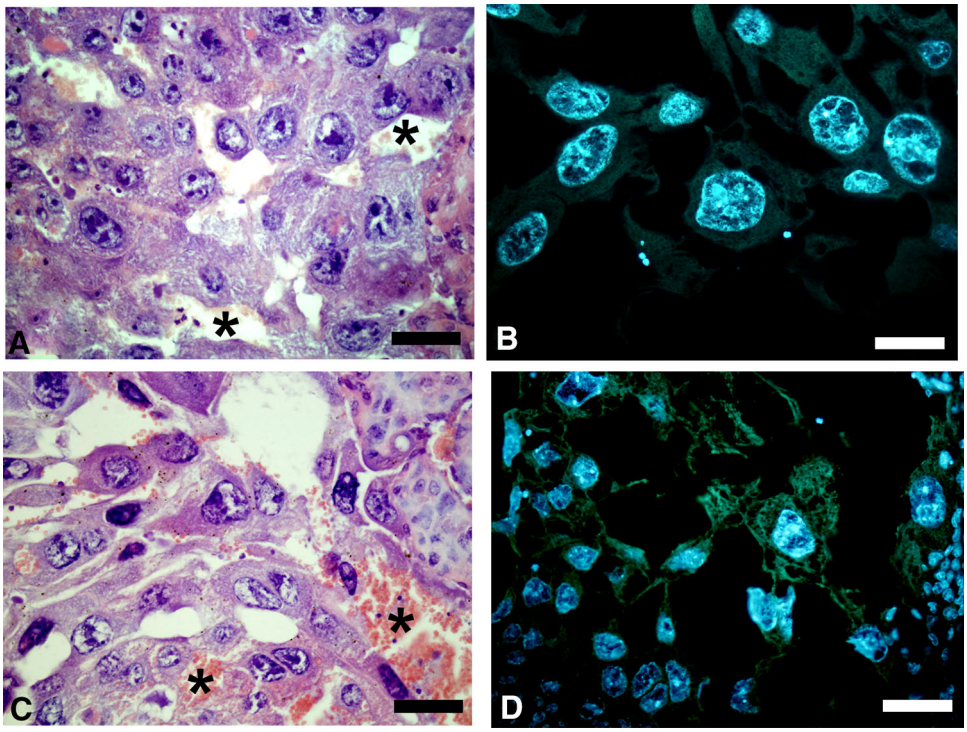

Fig. 3 Histological effects of perigestational alcohol intake on trophoblastic tissues. Histology (H-E) and nuclear morphology (*Hoechst 33,342*) of trophoblast from E10-IS of control (CF) and ethanol-treated females (TF). **a** Representative image of histological area section of trophoblast giant cell (TGC) layer from CF. **b** Nuclear morphology of TGC from CF. **c** Representative image of histological TGC layer from TF, showing increased spaces of maternal blood lacunae between smaller, irregular, and pycnotic TGCs. **d** Representative image of altered nuclear morphology of TGC layer from TF (*scale bar* **a–d**: 20 μm)

Table 3 Nuclear morphology of trophoblast giant cells (TGC) after perigestational alcohol intake

	Control females	Ethanol-treated females
Total TGC Nr	131	214
Normal TGC-nuclear Nr (frequency)	95 (72.5%)	134 (62.6%)*
Fragmented TGC-nuclear Nr (frequency)	6 (4.5%)	18 (8.4%)
Chromatin-condensed TGC-nuclear Nr (frequency)	99 (75.5%)	156 (72.8%)

The nuclear morphology of trophoblast giant cells (TGCs) from E10-implantation sites, was evaluated by *Hoechst 33,342* staining. The number (Nr) and frequency (%) of normal (ovoid and regular shaped) and fragmented nuclei or with chromatin condensed, were quantified in 4 images of the TGC-area per 2 implantation sites per female with a total of 5 females for control and ethanol-treated group

* $p < 0.05$, compared to controls, Fisher's exact test

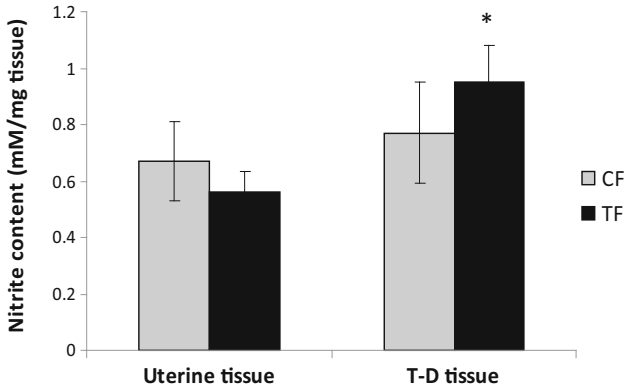

Fig. 4 Nitrite content in uterine myometrial and trophoblast-decidual tissues from control and ethanol-treated females. Total nitrite (NO_2) content (μM/mg prot) in myometrial and T-D tissues was determined as described in M–M. Data are expressed as mean ± SD for control (CF) and ethanol-treated females (TF). Number of myometrial samples per experimental group = 5; number of T-D tissue samples per experimental group = 10. *$p < 0.05$ compared to control, Student's *t*-test

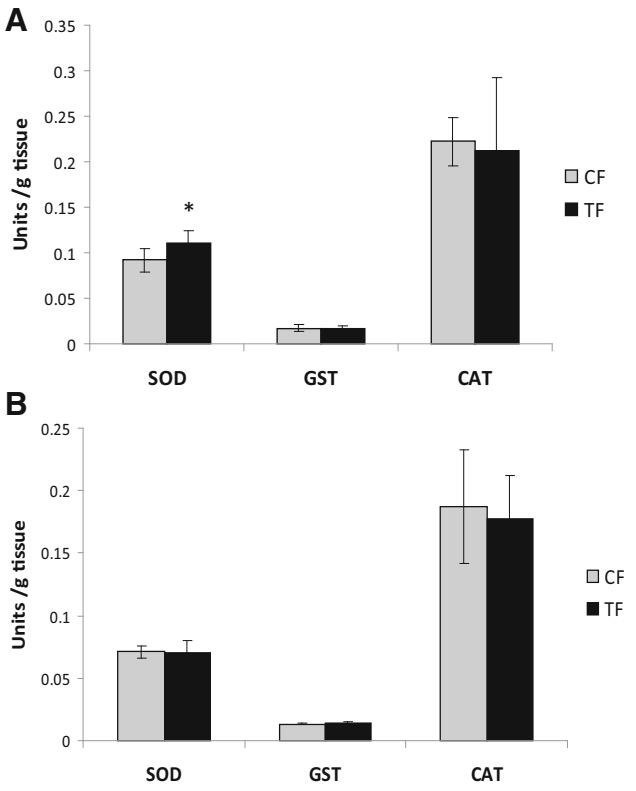

Fig. 5 Antioxidant enzymatic activities in uterine myometrial and trophoblast-decidual tissues after perigestational alcohol ingestion. Uterine myometrial (**a**) and trophoblast-decidual (**b**) tissues, dissected from implantation sites from control (CF) and treated females (TF), were prepared for measurement of antioxidant enzymatic activities of SOD, GST, and CAT. *Values* were expressed as mean Units/g ± SD. Number of uterine myometrial samples per experimental group = 5; number of T-D samples per experimental group = 10. *$p < 0.05$ versus control samples (Student's *t*-test)

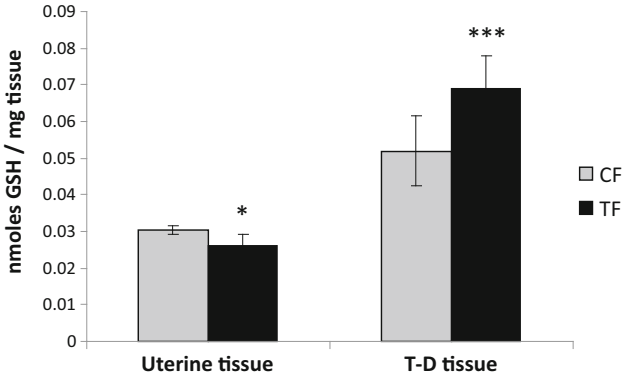

Fig. 6 Antioxidant non-enzymatic GSH content in uterine myometrial and trophoblast-decidual tissues after perigestational alcohol ingestion. Reduced glutathione (GSH) content (nmol/mg tissue) in explants of myometrium and trophoblast-decidual tissue of E10-implantation sites from control (CF) and treated females (TF). Data are expressed as mean nmol/mg tissue ± SD. Number of myometrial samples per experimental group = 5; number of T-D tissue samples per experimental group = 10. *$p < 0.05$; ***$p < 0.001$, compared to controls, Student's *t*-test

area from treated female mice was significantly larger than in controls ($p < 0.05$).

Discussion

We have previously shown that moderate alcohol ingestion before mating and up to day 10 of pregnancy, while producing no changes in calorie intake or body weight and with a blood alcohol concentration of 24.5 mg/dl, leads to reduced embryo growth and delayed development of advanced organogenic exposed embryos [31]. Our hypothesis was that perigestational alcohol intake in the outbred CF-1 mouse at organogenesis negatively affects maternal-placental tissues by an oxidative stress mechanism, generating lipid peroxidation, protein nitration, increased apoptosis, and histo-morphological alterations that can be the causes of altered embryogenesis at mid-gestation.

Intrauterine growth restriction is a key feature of FASD that may be associated with altered placenta formation. Previously, we showed that perigestational ethanol exposure impairs embryo development and growth at organogenesis, and now we demonstrated that placentation was disrupted at the maternal–fetal interface. Ethanol exposure produced alterations in the morphology of the labyrinthine zone and inhibited physiological transformation of maternal arteries. These findings concord with other studies in which pregnant Long-Evans dams fed isocaloric liquid diets containing 8% and higher % ethanol from gestation day 6–18, impairs fetal development and placental morphology [9]. However, experimental studies

Table 4 TBARS content in uterine and trophoblast-decidual tissues after perigestational alcohol ingestion at day 10 of gestation

Group	Uterine tissue (nmol TBARS/mg tissue)	T-D tissue (nmol TBARS/mg tissue)
Control females	6.30 ± 1.07	9.73 ± 1.00
Ethanol-treated females	5.69 ± 0.95	11.20 ± 0.81***

On day 10 of gestation, the uterine myometrial and trophoblast-decidual (T-D) tissues were dissected from E10-implantation sites from control and ethanol-treated females. The content of TBARS was tested in a total of $n = 5$ samples of uterine myometrial tissue and $n = 10$ samples of trophoblast-decidual tissue from at least 5 females per group. Data are expressed as mean value ± SD

*** $p < 0.001$ versus control, Student's *t*-test

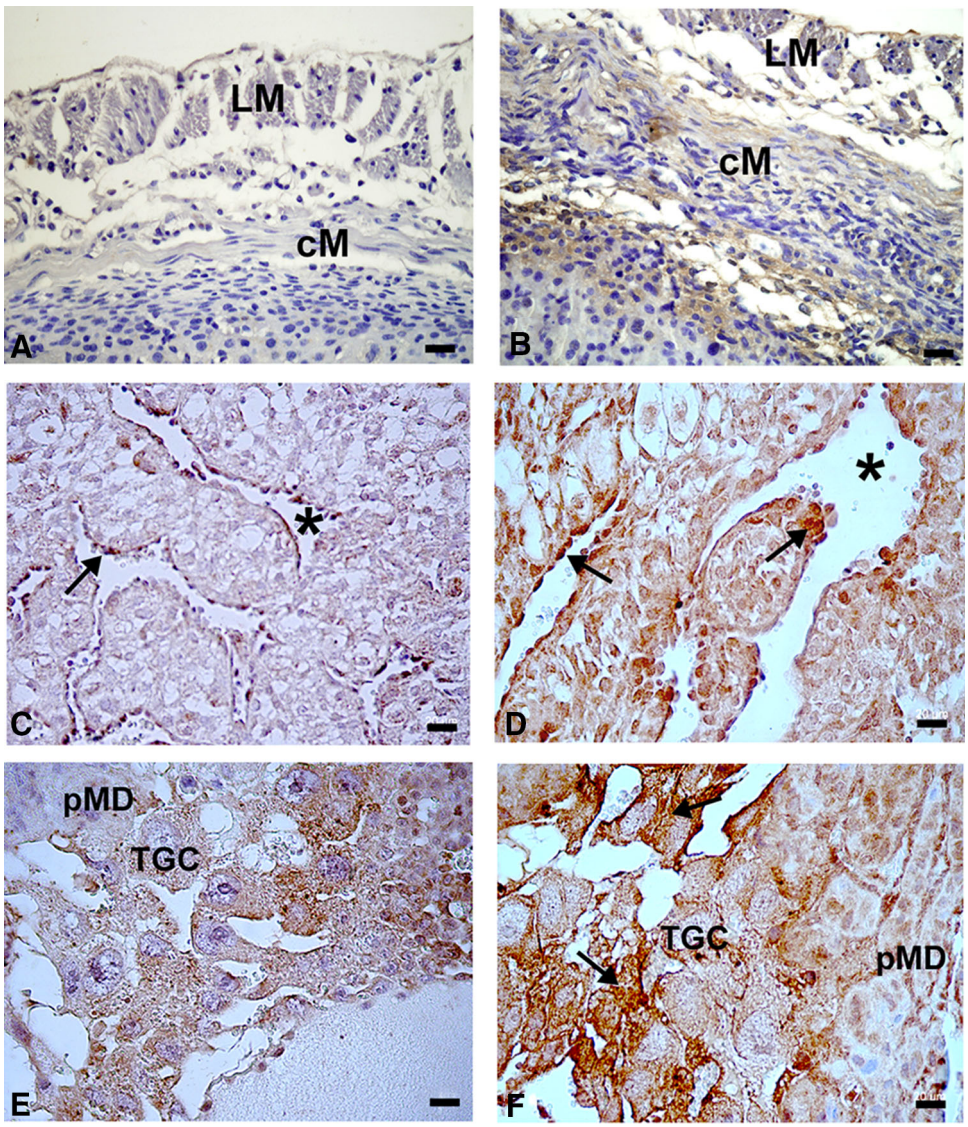

Fig. 7 Nitrotyrosine immunoexpression in myometrial and trophoblast-decidual tissues after perigestational alcohol intake. Representative photomicrographs of nitrotyrosine immunostained areas of myometrium (**a**, **b**), proximal mesometrial decidua (**c**, **d**), and trophoblast giant cell (TGC) layer of E10-IS from control (CF; **a**, **c**, **e**) and ethanol-treated females (TF; **b**, **d**, **f**). Myometrium of TF had very slight or almost negative immunoreaction for nitrotyrosine (3-NT) compared to the tissue of CF (**b** vs. **a**, respectively). Endothelial (*arrow*) and decidual cells of proximal decidua from TF presented strong 3-NT immunoreaction compared to the tissue of CF (**d** vs. **c**). The TGC layer of TF presented intense immunoreaction for 3-NT compared to control samples (**f** vs. **e**). *De* decidua, *TGC* trophoblast giant cells. *LM* longitudinal myometrium, *cM* circular myometrium (*scale bar* **a**–**f**: 20 μm)

were performed in inbred animal models and have been oriented toward high toxicological doses [39]. Also, data available from studies of alcohol-exposed pregnancies and effects on placentation are still limited. Most studies used in vitro studies of placentas of women whose inaccurate reporting of previous alcohol exposure, especially in the early stages of gestation, may be a source of considerable potential imprecision. This is a significant concern since rates of PAE in early pregnancy may involve nearly 40% of all pregnancies [4]. Our present study contributes to understanding of prenatal alcohol effects of a relevant dose/concentration of ethanol, commonly used by women,

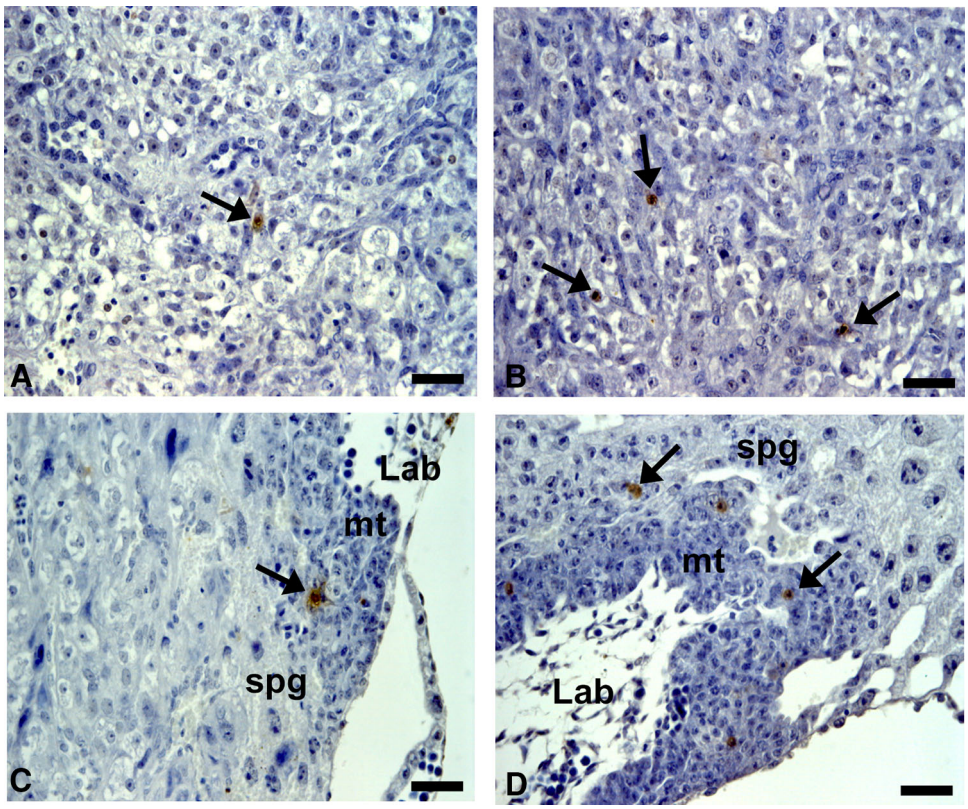

Fig. 8 Effects of perigestational alcohol intake on apoptotic index of trophoblast-decidual tissues. Representative images of apoptotic cells in mesometrial decidua (**a**, **b**) and in the trophoblastic zone (**c**, **d**). Note the increased frequency of TUNEL-positive cells (*arrow*) in the decidua of treated females (TF) (**b**) compared to the frequency in decidual tissue of control females (CF) (**a**). In the area of trophoblastic cells, increment of TUNEL-positive cell frequency was observed mainly in the mononuclear trophoblast (mt) cells of TF (**d**), in comparison to frequency of TUNEL-positive trophoblast cells found in CF (**c**). *Arrow* TUNEL-positive cells. *Lab* labyrinth. *Spg* spongiotrophoblast layer (*scale bar* **a**–**d**: 20 μm)

Table 5 Apoptotic index in uterine and trophoblast-decidual tissues after perigestational alcohol intake

Group	Decidual tissue (mean apoptotic cell Nr ± SD)	Trophoblastic tissue (mean apoptotic cell Nr ± SD)
Control females	1.3 ± 0.8	17.0 ± 3.2
Ethanol-treated females	2.6 ± 1.1*	37.1 ± 6.6*

The apoptotic index was determined in E10-implantation site by TUNEL assay. The mean number of TUNEL-positive cells ± SD was assessed in mesometrial decidua and in trophoblastic tissue, including the TGC, spongiotrophoblast, mononuclear, and chorionic trophoblast cells, in a total of 10 sections of implantation sites from 5 female mice for each group

* $p < 0.05$, versus control, Student's *t*-test

on early placentation. The CF-1-treated females, in the present model, consumed about 0.5 g ethanol/mouse, equivalent to 35–40 g ethanol in humans, considering that daily consumption of 0.22 g ethanol/male rat is equivalent to 18 g ethanol/human male consumption [40]. In humans, this concentration of ethanol consumption is produced by the ingestion of two glasses of wine containing 11% of ethanol, distributed throughout the day, a total of 200 ml of wine/day [40]. According to this value of ethanol consumption, our model is within the range of moderate drinkers. However, the value of BAC produced in CF-1-treated mice, was 22–24 mg % which corresponds to a low alcohol drinker. Increased risk (4.3% of women) of placental abruption with the consumption of 7–21 drinks per week was reported [4] (a mean of two drinks per day and BAC of 5–100 mg/dl). In our study, although a low BAC was detected, we showed decidual and placental alcohol disruption, suggesting that these alterations may be involvement in early retarded and abnormal embryogenesis at organogenesis. These deleterious early effects probably conduct to abnormal fetal development and growth at perinatal stage. At this respect, some studies reported an increase of babies with low birth weight from women that drank 14 or more drinks per week (about two glasses of wine 11% per day or 18–30 g absolute ethanol/day), while thirteen of the 35 women (37%) who consumed more than 100 g of ethanol per week (14 g absolute ethanol/day) gave birth to children with FAS [4].

Our main hypothesis was that perigestational alcohol consumption up to day 10 of gestation induced oxidative

stress in uterine and decidual-trophoblast tissues. In the uterine myometrium of implantation site from treated females, increased SOD activity and decreased GSH content suggest oxidative stress induction. Since the SO anion is detoxified by SOD enzymes, elevated SOD activity may indicate its induction caused by increased ROS in tissue. However, although NO production was not found to be higher, decreased GSH level suggests its consumption to recompose redox balance in the myometrium. In this case, the uterus was able to neutralize ethanol-induced ROS generation by SOD activation and GSH/GSSH system, which resulted in no changes in TBARS content in tissue. Activation of SOD and consumption of GSH could be sufficient to avoid activation of the other antioxidant enzymes determined herein whose activities remained constant. Therefore, no increment of protein nitrosylation, lipid peroxidation, or DNA damage by apoptosis was found in uterine tissue after the present ethanol treatment.

In the trophoblast-decidual tissue, perigestational alcohol ingestion yields to an increment of GSH level suggesting that reactive oxygen species are generating in these tissues. Oxidative stress was also observed in the villi of human placenta after alcohol consumption [14, 16]. However, contrary to expectations, antioxidant CAT, SOD, and GST activities were unchanged in this tissue, compared to the levels of antioxidant enzymatic defenses of maternal-placental tissues from controls. Maternal alcohol consumption of more than three drinks per occasion produces prominent systemic OS. Postpartum subjects demonstrated a marked reduction of systemic GSH, along with significant increases in the percentage of oxidized GSSG and oxidation of the GSH redox potential [41]. Perhaps the present ethanol dose was not sufficient to induce changes in enzymatic antioxidant defenses, although a strong response in the level of GSH was generated, indicating oxidative stress.

Perigestational alcohol-induced OS leads to altered cell structures and tissue damage in decidual–placental interface from increased apoptosis, lipid peroxidation, and protein nitration. In decidua, detachment of endothelial cells towards the blood space and the presence of multifocal parenchymal thrombi within maternal vessels were observed in ethanol-exposed implantation sites. The diminished vascular lumen of spiral arteriolar vessels may lead to vasoconstriction, an effect that can explain the reduced total area of the implantation site observed. Histological alterations of decidua found in the present ethanol treatment were similar to others observed in placental tissue after alcohol exposure [16, 42]. Moreover, other authors observed that pregnant Long-Evans rats, fed 37% of ethanol-derived calories in liquid diets from gestational days 6–16 presented reduced thickness of the placenta [9, 17]. Perhaps perigestational alcohol ingestion up to day 10 of gestation leads to hypoxia–ischemia of maternal and placental tissues, suggesting that this mechanism is able to induce the release of ROS in the tissue. Similarly to the present ethanol model, in which maternal blood lumen of decidual vessels was reduced, poor vascularization and arteriolar vasoconstriction of maternal blood vessels can be the cause of extended hypoxic state and generation of ROS and NO release in the exposed placental tissue [42, 43]. In addition, reduced decidual vascular lumen and hypoxia could induce high expression and activity of endothelial nitric oxide synthase (eNOS) in which case increased NO levels are generated in decidual tissue, as suggested by others [44]. Alterations in NO production depend on the level and length of ethanol exposure. Chronic and/or acute ethanol intake increases the concentration of total nitrites in serum of ethanol-treated animals [45] and in patients with chronic liver disease [46]. In low doses, ethanol also increases the activities of NO and eNOS, augmenting endothelial vasodilation [19]. Thus, cell-tissue damage may result from high NO and peroxynitrite production during NO–SO interaction under oxidative conditions [47]. Hence, NO, contributing to the generation of RNS could be an important factor contributing to the morpho-functional alterations of vascularization of maternal-placental tissues in ethanol-exposed females.

Together with decidual histological alterations, the trophoblast layer of the implantation sites from perigestational alcohol-treated females was also affected. Although a non-increased number of trophoblast nuclei with fragmented or chromatin condensation was observed, the nucleus of trophoblast giant cells from the exposed implantation sites was altered. Also, similar to what occurs in decidua, the spongiotrophoblastic layer from treated females has sinusoids with reduced maternal blood spaces. As a consequence, a high and/or persistent hypoxic state in this layer, opposed to normoxia that occurs at the maternal–placental interface around day 10 of gestation, may generate placental OS and deterioration of the syncytiotrophoblast interface. These ethanol effects may give rise to a variety of complications including miscarriage, recurrent pregnancy loss, and IUGR, among others [12].

NO reacts strongly with the superoxide anion to generate peroxynitrite radical, which causes damage to lipids, proteins [48], and DNA [49]. Although in alcohol-exposed myometrial tissue TBARS content was not increased, TBARS content in trophoblast-decidual tissue from treated females was higher than in controls. This mechanism could be one of the main factors in placental damage during organogenesis. Also, excess nitration of tyrosine [14] can affect the structure and function of proteins [50, 51]. In our mouse model of alcohol exposure, the altered histo-morphology of trophoblast-decidual tissue could be due, at

least in part, to protein nitrosylation and increased peroxynitrites. Peroxynitrite has been shown to disorganize actin polymerization through actin nitration [50], and to disrupt microtubules of the intestinal barrier [51]. Similar to our model, nitration of fetal vasculature and villous strome was also observed in pre-eclamptic and diabetic placentas [12, 52]. However, once the level of cellular damage inflicted when peroxynitrite exceeds any possibility of repair, the cell eventually dies via apoptosis or necrosis. Apoptosis increases progressively with advancing gestation until delivery [53], playing an important role in cellular homeostasis, placental tissue remodeling, trophoblast differentiation, growth, and degeneration. Both morphology and function of the placenta depend on an adequate balance between proliferation, differentiation, and apoptosis. In the present model for perigestational alcohol intake, a high apoptotic index was observed in the decidual tissue and trophoblastic layer, probably related to excess NO production, which leads to high protein nitration and lipid peroxidation [54]. In particular, although the chorionic trophoblast cells in the labyrinth did not present obvious histo-morphological alterations, this layer was the most affected in terms of the level of apoptosis at organogenesis. However, long-term apoptotic effects in this layer may lead to placental alterations that potentially culminate in abortion, premature birth, growth restriction, and other complications [55].

In conclusion, in this work, the elucidation of the cellular and molecular effects and mechanisms, involved in alcohol-induced in placentophaty after moderate maternal alcohol exposure up to early pregnancy, may be useful for identification of risk molecular factors for early abnormal placentation and defective mechanisms that can induce birth growth disorders and defects. Thus, different oxidative stress status was demonstrated to be induced in myometrium or trophoblast-decidual tissue after perigestational alcohol intake in CF-1 mouse at organogenesis. The decidual–placental interface was more susceptible to OS mechanisms than uterine tissue, since altered macromolecules and cells of this tissue may lead to the main pathophysiological features observed in the implantation sites from ethanol-exposed female mice at organogenesis. The present results may lead to further studies to find earlier and appropriate interventions during pregnancy to mitigate the adverse effects of maternal alcohol consumption at early gestation that can lead to fetal alcohol spectrum disorders.

Acknowledgements This work was supported by the Consejo Nacional de Investigaciones Científicas y Técnicas (CONICET) (PIP-CONICET, Grant Numbers: 114-200801-00014 and 11220090100 492); the Agencia Nacional de Promoción Científica y Tecnológica (Grant Number BID-PICT-2008-2210); and the Universidad de Buenos Aires, Argentina (Grant Number UBACyT X187). The authors are very grateful to Dr. Cristian Sobarzo for his technical assistance in confecting the figures.

Compliance with ethical standards

Conflicts of interest The author(s) declare that they have no potential conflicts of interest with respect to the research, authorship, and/or publication of this article.

References

1. Jones KL, Smith DW, Ulleland CN et al (1973) Pattern of malformations in offspring of chronic alcoholic mothers. Lancet 1:267–271
2. Guerri C, Bazinet A, Riley EP (2009) Foetal alcohol spectrum disorders and alterations in brain and behaviour. Alcohol Alcohol 44(2):108–114
3. May PA, Gossage JP (2011) Maternal risk factors for fetal alcohol spectrum disorders: not as simple as it might seem. Alcohol Res Health 34(1):15–26
4. Burd L, Roberts D, Olson M, Odendaal HJ (2007) Ethanol and the placenta: a review. Materrn Fetal Neonatal Med 20(5):361–375
5. Roozen S, Peters GJ, Kok G, Townend D, Nijhuis J, Curfs L (2016) Worldwide prevalence of fetal alcohol spectrum disorders: a systematic literature review including meta-analysis. Alcohol Clin Exp Res 40(1):18–32
6. Popova S, Lange S, Probst C, Gmel G, Rehm J (2017) Estimation of national, regional, and global prevalence of alcohol use during pregnancy and fetal alcohol syndrome: a systematic review and meta-analysis. Lancet Glob Health. doi:10.1016/S2214-109X(17)30021-9
7. Bosco C, Diaz E (2012) Pharmacology and cell metabolism. Placental hypoxia and foetal development versus alcohol exposure in pregnancy. Alcohol Alcoholism 47(2):109–117
8. Burd L, Hofer R (2008) Biomarkers for detection of prenatal alcohol exposure: a critical review of fatty acid ethyl esters in meconium. Birth Defects Res A Clin Mol Teratol 82(7):487–493
9. Gundogan F, Gilligan J, Qi W, Chen E, Naram R, de la Monte SM (2015) Dose effect of gestational ethanol exposure on placentation and fetal Growth. Placenta 36:523–530
10. Xu Y, Xiao R, Li Y (2005) Effect of ethanol on the development of visceral yolk sac. Hum Reprod 20(9):2509–2516
11. Adamson SL, Lu Y, Whiteley KJ, Holmyard D, Hemberger M, Pfarrer C, Cross J (2002) Interactions between trophoblast cells and the maternal and fetal circulation in the mouse placenta. Dev Biol 250(2):358–373
12. Agarwal A, Aponte-Mellado A, Premkumar BJ, Shaman A, Gupta S (2012) The effects of oxidative stress on female reproduction: a review. Reprod Biol Endocrin 10:49–79
13. Lappas M, Hiden U, Desoye G, Froehlich J, Hauguel-de Mouzon S, Jawerbaum A (2011) The role of oxidative stress in the pathophysiology of gestational diabetes mellitus. Antioxid Redox Signal 15(12):3061–3100
14. Webster RP, Roberts VHJ, Myatt L (2008) Protein nitration in placenta—functional significance. Placenta 29:985–994
15. Myatt L (2010) Review: reactive oxygen and nitrogen species and functional adaptation of the placenta. Placenta. doi: 10.1016/j.placenta.2009.12.021

16. Kay HH, Grindle KM, Magness RR (2000) Ethanol exposure induces oxidative stress and impairs nitric oxide availability in the human placental villi: a possible mechanism of toxicity. Am J Obstet Gynecol 182:682–688
17. Gundogan F, Elwood G, Mark P et al (2010) Ethanol-induced oxidative stress and mitochondrial dysfunction in rat placenta: relevance to pregnancy loss. Alcohol Clin Exp Res 34:415–423
18. Rahal A, Kumar A, Singh V, Yadav B, Tiwari R, Chakraborty S, Dhama K (2014) Oxidative stress, prooxidants, and antioxidants: the interplay. Biomed Res Int. - 2014:761264
19. Deng XS, Deitrich RA (2007) Ethanol metabolism and effects: nitric oxide and its interaction. Curr Clin Pharmacol 2:145–153
20. Kovacic P (2005) Unifying mechanism for addiction and toxicity of abused drugs with application to dopamine and glutamate mediators: electron transfer and reactive oxygen species. Med Hypotheses 65:90–96
21. Myatt L, Cui X (2004) Oxidative stress in the placenta. Histochem Cell Biol 122:369–382
22. Fujii J, Iuchi Y, Okada F (2005) Fundamental roles of reactive oxygen species and protective mechanisms in the female reproductive system. Reprod Biol Endocrinol 3:43
23. Chandra A, Surti N, Kesavan S, Agarwal A (2009) Significance of oxidative stress in human reproduction. Arch Med 5:528–542
24. Rosselli M, Keller PJ, Dubey RK (1998) Role of nitric oxide in the biology, physiology and pathophysiology of reproduction. Hum Reprod Update 4:3–24
25. Birben E, Sahiner UM, Sackesen C, Erzurum S, Kalayci O (2012) Oxidative stress and antioxidant defense. WAO J 5:9–19
26. Mate´s JM (2000) Effects of antioxidant enzymes in the molecular control of reactive oxygen species toxicology. Toxicology 153:83–104
27. Halliwell B (2006) Reactive species and antioxidants. Redox biology is a fundamental theme of aerobic life. Plant Physiol 141:312–322
28. Devi BG, Schenker S, Mazloum B, Henderson GI (1996) Ethanol-induced oxidative stress and enzymatic defenses in cultured fetal rat hepatocytes. Alcohol 13:327–332
29. Floyd RL, Decofle P, Hungerfond DW (1999) Alcohol use prior to pregnancy recognition. Am J Prev Med 12:101–107
30. Cebral E, Faletti AB, Jawerbaum A, Paz DA (2007) Periconceptional alcohol consumption-induced changes in embryonic prostaglandin E levels in mouse organogenesis. Modulation by nitric oxide. Prost Leuk Ess Fatty Ac 76:141–151
31. Coll TA, Perez-Tito L, Sobarzo CMA, Cebral E (2011) Embryo developmental disruption during organogenesis produced by CF-1 murine periconceptional alcohol consumption. Birth Defects Res B 92:560–574
32. Coll TA, Chaufan G, Pérez-Tito L, Ventureira MR, Sobarzo CMA, de Molina Ríos, MdC Cebral E (2017) Oxidative stress and cellular and tissue damage in organogenic outbred mouse embryos after moderate perigestational alcohol intake. Mol Reprod Dev. doi:10.1002/mrd.22865
33. Aebi H (1984) Catalase in vitro. Methods Enzymol 105:121–126
34. Habig WH, Pabst MJ, Jakoby WB (1976) Glutathione S-transferase a from rat liver. Arch Biochem Biophys 75(2):710–716
35. Beauchamp C, Fridovich IJ (1971) Superoxide dismutase: improved assays and an assay applicable to polyacrylamide gels. Anal Biochem 44(1):276–286
36. Anderson ME (1985) Determination of glutathione and glutathione disulfide in biological samples. Methods Enzymol 113:548–553
37. Beuge JA, Aust SD (1978) Microsomal lipid peroxidation. Methods Enzymol 52:302–310
38. Green LC, Wagner DA, Glogowski J, Skipper PL, Wishnok JS, Tannenbaum SR (1982) Analysis of nitrate, nitrite and [15 N] nitrate in biological fluids. Anal Biochem 126:131–138
39. McDonough KH (2003) Antioxidant nutrients and alcohol. Toxicology 189:89–97
40. Gonzalez Martín C, Vega Agapito V, Obeso A, Prieto-Lloret J, Bustamante R, Castañeda J, Agapito T, Gonzalez C (2011) Moderate ethanol ingestion, redox status, and cardiovascular system in the rat. Alcohol 45:381–391
41. Gauthier TW, Kable JA, Burwell L, Coles CD, Brown LA (2010) Maternal alcohol use during pregnancy causes systemic oxidation of the glutathione redox system. Alcohol Clin Exp Res 34:123–130
42. Acevedo CG, Carrasco G, Burotto M, Rojas S, Bravo I (2001) Ethanol inhibits L-arginine uptake and enhances NO formation in human placenta. Life Sci 68:2893–2903
43. Wareing M, Greenwood SL, Baker PN (2006) Reactivity of human placental chorionic plate vessels is modified by level of oxygenation: differences between arteries and veins. Placenta 27:42–48
44. Kimura H, Weisz A, Kurashima Y, Hashimoto K, Ogura T, D'Acquisto F, Addeo R, Makuuchi M, Esumi H (2000) Hypoxia response element of the human vascular endothelial growth factor gene mediates transcriptional regulation by nitric oxide: control of hypoxia inducible factor-1 activity by nitric oxide. Blood 95:189–197
45. Baraona E, Shoichet L, Navder K, y Lieber CS (2002) Mediation by nitric oxide of the stimulatory effects of ethanol on blood flow. Life Sci 70:2987–2995
46. Oekonomaki E, Notas G, Mouzas I, Valatas V, Skordilis P, Xidakis C, Kouroumalis E (2004) Binge drinking and nitric oxide metabolites in chronic liver disease. Alcohol Alcohol 39:106–9
47. Cooper RG, Magwere T (2008) Nitric oxide-mediated pathogenesis during nicotine and alcohol consumption. Indian J Physiol Pharmacol 52:11–18
48. Spiteller G (2006) Peroxyl radicals: inductors of neurodegenerative and other inflammatory diseases. Their origin and how they transform cholesterol, phospholipids, plasmalogens, polyunsaturated fatty acids, sugars, and proteins into deleterious products. Free Rad Biol Med 41:362–387
49. Plachta N, Traister A, Weil M (2003) Nitric oxide is involved in establishing the balance between cell cycle progression and cell death in the developing neural tube. Exp Cell Res 288:354–362
50. Kasina S, Rizwani W, Radhika KV et al (2005) Nitration of profilin effects its interaction with poly (L-proline) and actin. J Biochem 138:687–695
51. Banan A, Fields JZ, Decker H, Zhang Y, Keshavarzian A (2000) Nitric oxide and its metabolites mediate ethanol-induced microtubule disruption and intestinal barrier dysfunction. J Pharmacol Exp Ther 294:997–1008
52. Jawerbaum A (2016) Placental endoplasmic reticulum stress and acidosis: relevant aspects in gestational diabetes. Diabetologia 59 (10):2080–2081
53. Smith SC, Baker PN, Symonds EM (1997) Placental apoptosis in normal human pregnancy. Am J Obstet Gynecol 177:57–65
54. Zingarelli B, O'Connor M, Wong H, Salzman AL, Szabo C (1996) Peroxynitrite-mediated DNA strand breakage activates poly-adenosine diphosphate ribosyl synthetase and causes cellular energy depletion in macrophages stimulated with bacterial lipopolysaccharide. J Immunol 156:350–358
55. Crocker IP, Cooper S, Ong SC, Baker PN (2003) Differences in apoptotic susceptibility of cytotrophoblasts and syncytiotrophoblasts in normal pregnancy to those complicated with preeclampsia and intrauterine growth restriction. Am J Pathol 162:637–643